Journal of Stress Analysis
Vol. 3, No. 1, Spring – Summer 2018
Bu-Ali Sina University

An Experimental Investigation into Wear Resistance of Mg-SiC Nanocomposite Produced at High Rate of Compaction

G.H. Majzoobi[a,*], K. Rahmani[a], A. Atrian[b]

[a]Mechanical Engineering Department, Bu-Ali Sina University, Hamedan, Iran.

[b]Mechanical Engineering Department, Najafabad Branch, Islamic Azad University, Najafabad, Iran.

Article info

Article history:
Received 27 April 2018
Received in revised form
19 September 2018
Accepted 20 September 2018

Keywords:
SiC
Nanocomposite
Powder metallurgy
Dynamic compaction
Wear

Abstract

The Mg-SiC nanocomposite specimens were produced at low strain rate of $8\times10^{-3}s^{-1}$ using a universal INSTRON testing machine, strain rate of about $8\times10^{2}s^{-1}$ using a drop hammer and at strain rate of about $1.6\times10^{3}s^{-1}$ employing a Split Hopkinson Pressure Bar (SHPB). Tribological behavior of the samples was investigated in this work. The compaction process was performed at the temperature of 723K. The results showed increase in the wear resistance as the nano reinforcement increased. The results also indicated that as the reinforcement content increased to 10 vol%, the weight loss reduced approximately by 63%, 58%, and 35% for the samples fabricated by SHPB, drop hammer, and quasi-static hot pressing, respectively. The results also suggested that the wear rate of samples fabricated by SHPB was nearly 40% lower than that for quasi-statically fabricated samples and non-reinforced samples.

1. Introduction

Particulates reinforced Mg matrix composites (MMCs) have increasingly found application in aerospace and automotive industries. Concurrent demands on high wear resistance and weight reduction in automotive industries have motivated researchers to perform various studies on MMCs [1-7]. The literature suggests that the wear resistance and strength of Mg and its alloys can be enhanced by reinforcing them with ceramic particles, such as Al_2O_3, SiC, MgO, TiC, B_4C, TiB_2, and ZnO [8].

In most powder metallurgy (PM) techniques, the compaction is performed quasi-statically whereas in some cases the compaction is carried out at high rate of loading. Hot pressing [9], hot isostatic pressing [10], and mechanical milling, and hot extrusion [11, 12] are typical examples of techniques in which the compaction loads are applied quasi-statically. High rate of compactions [13, 14] are accomplished through dynamic loading or shock wave loadings [15]. In latter techniques, some devices like dropping hammer or explosive-compressed gas accelerated projectile are used for compaction. The main advantage of high rate consolidation methods is that hot sintering is primarily not necessary for compaction. In exchange, the impact energy usually supplies the high local temperature rise at the powder particle interfaces which is adequate for local metallurgical bonding. Therefore, during dynamic compaction, the microstructural changes like grain coarsening and particles aggregation can be minimized [16].

Several researchers such as Thakur et al. [17] and Francis et al. [18] have studied quasi-static com-

*Corresponding author: G.H. Majzoobi (Professor)
E-mail address: gh_majzoobi@basu.ac.ir
http://dx.doi.org/10.22084/jrstan.2018.16240.1048
ISSN: 2588-2597

paction. Jiang et al. [19] investigated the feasibility of the fabrication of B_4C particulates reinforced Mg by powder metallurgy (PM) technique. Wang et al. [20] and Yan et al. [21] also applied impact energy for compaction of powder materials. Faruqui et al. [22] produced Mg-SiC composites using mechanical milling and underwater shock consolidation. Atrian et al. [23] presented a comparative study on dynamic compaction and quasi-static hot pressing for fabrication of Al7075-SiC nanocomposite. Majzoobi et al. [24] also produced Al7075-B_4C composite by some techniques with various densification rates [23, 25].

There are several studies on the effects of SiC particles on the wear properties of Mg and its alloys. For example, Lim et al. [3] reported slight improvement in the wear resistance of AZ91 alloy reinforced with 8 vol% SiC (particle size of 14μm) under the load of 10N. Thakur and Dhindaw [2] also obtained that well-dispersed SiC particles may lead to higher wear resistance and lower friction coefficient (FC) in Al and Mg metals. Similar results were also presented by Lim et al. [3]. Further improvement of tribological properties encouraged some researchers to incorporate nano reinforcements into pure Mg [4, 5]. Mondal and Kumar [26] observed decreased wear rate of AE42 Mg alloy hybrid composites reinforced with Saffil short fibers and SiC particles in comparison to the Saffilnshort fibers reinforced composite and unreinforced alloy. Umeda et al. [7] showed that carbon nanotubes (CNTs) and SiO_2 reinforcements could improve the wear tolerance and decrease the friction coefficient (FC) of hybrid composites. Majzoobi et al. [27] also studied the tribological properties and the wear mechanisms of dynamically compacted Al7075-SiC nanocomposite. In the current investigation, Mg-SiC nanocomposite was produced at high rate of loading using a SHPB and a drop hammer and at low rate of loading using an Instron universal testing machine. The main objective in this work was to explore the tribological properties and the wear mechanisms in the samples produced at various rate of loading.

2. Experiments

2.1. Materials and Fabrication of Samples

In this study, Mg powder with purity of 99.5% with particle size of 100 m (regular morphology) was used as matrix and SiC powder with purity of 99% and particle size of 75nm (spherical morphology) was used as reinforcing phase. Further information can be found in [13] and [14]. The specimens were produced using the SHPB and drop hammer (DH) described in the references [13] and [14], respectively. In order to investigate the effects of nanoparticle content, cylindrical nanocomposite samples (with diameter of 15mm and length of 11-12mm) with 0, 1.5, 3, 5 and 10% volume fraction of SiC were produced at the temperatures of 723K. The procedure of producing the samples can be found in [27] and [28].

2.2. Quasi-static Hot Pressing

Nanocomposite powder was hot pressed quasi-statically using an INSTRON universal testing machine. In order to have a proper compaction, it was required to calculate the optimum duration and the level of the pressure necessary to obtain the maximum density [23]. To do this, eight pure Mg specimens were produced at 723K and under the pressures of 300 and 600MPa for 5, 15, 25, and 35min time duration.

Fig. 1 illustrates the effect of pressure level and time duration on the density. As the figure suggests, the pressure of 600MPa gives the higher density and consequently, this pressure and its corresponding time duration (25min) were selected to produce the pure samples with 0-10 vol% SiC content.

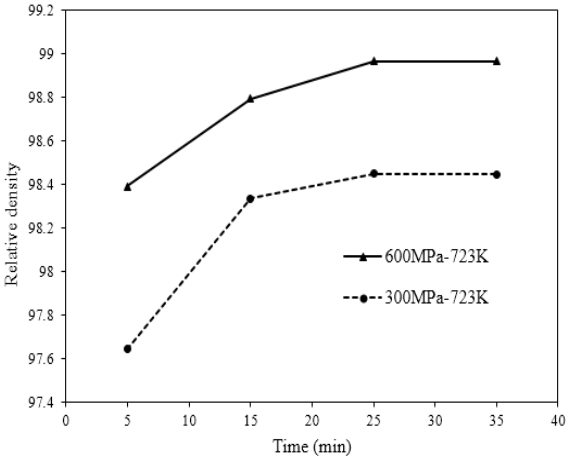

Fig. 1. Density-time histories for two compact pressure.

Therefore, the compaction tests were carried out at the rate of 5mm/min that corresponds to a strain rate of around $8.0\times10^{-3}s^{-1}$. To prevent from formation of void and pore, the pressure was released when temperature dropped below 573K [23].

2.3. Dynamic Compaction Using Drop Hammer

A mechanical drop hammer [14] was used for dynamic compaction of nanocomposite powders. The schematic view of the device is depicted in Fig. 2a. In this device, a 60kg weight is dropped from the height of 3.5m and hits the specimen at an impact velocity of around 8m/s (based on $v = \sqrt{2gh}$ equation). This impact speed corresponds to a strain rate of around $0.8\times10^{-3}s^{-1}$. The dropping hammer delivers around 2kJ energy ($E = Mv^2/2$) to the powder for compaction. As mentioned earlier, the compaction was performed at the temperature of 723K. Further details can be found in [14].

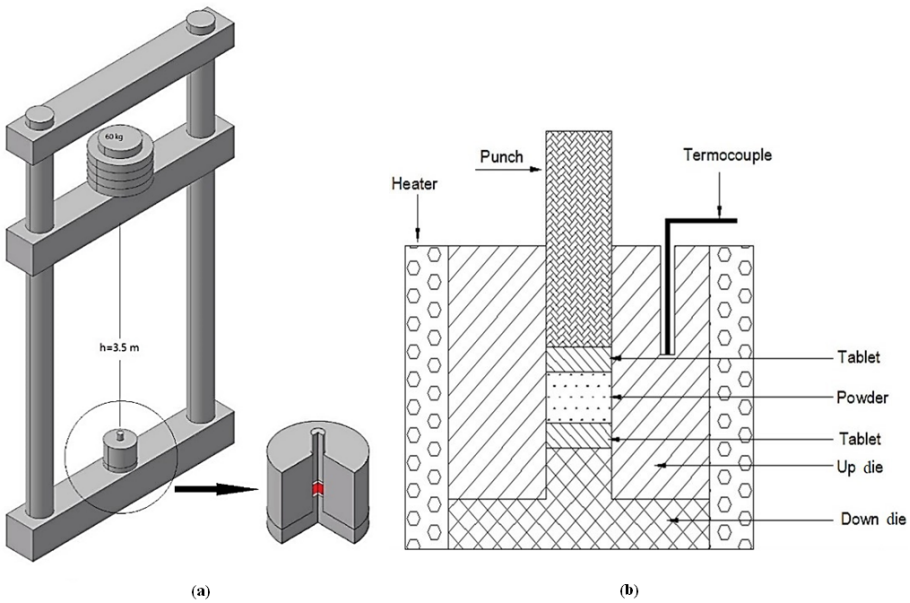

Fig. 2. The schematic views of (a) The drop hammer and (b) The die.

The schematic view of the die is shown in Fig. 2b. The die and the punch were made of Mo40 (1.7225) and VCN150 (1.6582) steel, respectively to resist against thermal and impacting loads. Two tablets (5mm length) of VCN150 steel were also mounted on top and beneath of powder to reduce the spring-back and to preserve the surface quality of the compact

The required temperature (maximum about 450°C) was supplied by a 1200W furnace. The impact on the powder was accomplished when the powder temperature reached a steady state. After compaction, the samples were ejected out of the die and were cooled at ambient temperature.

2.4. High Rate Compaction Utilizing SHPB

The high rate compactions were carried out utilizing a SHPB set up. Fig. 3 schematically depicts a SHPB, which consists of three bars; striker, incident (input), and transmitter (output). The input and output bars in the current research had a diameter of 40mm, length of 3m, and were made of a high strength steel alloy (Maraging steel) with an ultimate strength of about 1600MPa. In this set-up, mechanically milled Mg-SiC powder was poured in a die which had been mounted between the input and output bars of the SHPB. The set up geometry, its components and the compaction procedure are fully described in [13]. The compaction temperature was 723K for all experiments. The reason is explained in [13].

2.5. Characterizing Tests

To evaluate the effects of processing techniques, as well as the SiC reinforcement content on the samples hardness, the Vickers microhardness of compacted samples was measured. For microhardness measurement, a 100gf for 15s was applied to the specimen using a tetragonal indenter [29].

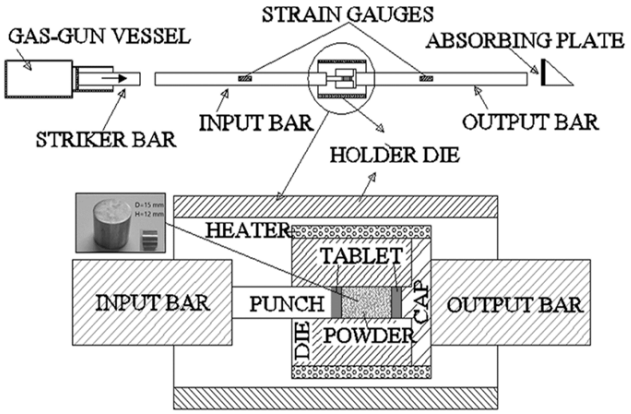

Fig. 3. The schematic view of the Split Hopkinson set-up with loading tool.

Dry sliding wear tests were performed utilizing a pin-on-disc test device shown in Fig. 4 according to ASTM G99 [30]. A pin-on-disc instrument was used to evaluate the wear loss as well as the friction coefficient. To this end, the compacted specimens with 15mm diameter were placed in a 30mm diameter disk-shape container. Before each test, the pin and sample surface were cleaned with acetone. All the tests were done on various applied loads of 10 and 20N with sliding speeds of 0.09m/s. To have a deeper insight into the matter, the wear tests were performed for two various sliding distances of 250 and 500m. After each test, the specimen and pin were cleaned with organic solvents to remove traces. The sample was weighted (accuracy of 0.1mg) before and after testing to determine the amount of wear loss.

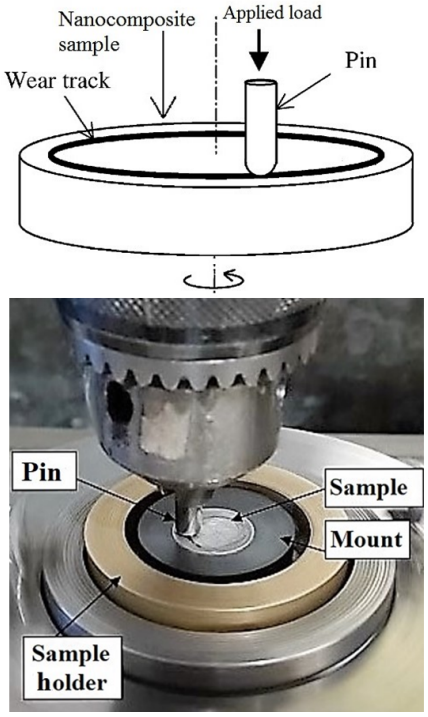

Fig. 4. Pin-on-disk wear mechanism.

3. Results and Discussion

3.1. Microhardeness

Variation of Vickers microhardness of fabricated specimens versus different amounts of SiC vol% for different compaction techniques is illustrated in Figure 5. As the figure implies, 10 vol% SiC reinforcement has increased the microhardness of the compacted samples fabricated using SHPB, drop hammer, and quasi-static pressing by around 45%, 32% and 28 %, respectively. Nano reinforcement enhances the hardness mainly due to its hardening effects and its intrinsic hardness [31]. Seetharama et al. [32], Jiang et al. [33] and Umeda et al. [7] also reported similar observations in their investigations. Higher micro-hardness of samples fabricated by SHPB was attributed to more severe work hardening and stronger bonding [34].

3.2. Wear Properties

3.2.1. Sliding Distance Effects

Variation of weight loss versus sliding distance under sliding speed of 0.09m/s and normal load of 20N is shown in Figure 6 for two various sliding distances of 250 and 500m. As it is observed, weight loss increases with increasing the sliding distance. The figure also shows the highest wear resistance for the samples fabricated using SHPB. It is also seen in the figure that the weight loss decreases as the reinforcement content increases. The weight loss of the compacted samples by SHPB decreases from about 1.17 to 0.43mg/m (63% reduction) when the SiC content increases from 0 to 10 vol%. The high wear resistance of Mg-SiC samples produced by SHPB can be attributed to its increased hardness and also to the strong bonding between the nanoreinforcement and Mg matrix that facilitates the load transfer from the matrix to the hard particles [22, 34]. This confirms the results provided by Wang et al. [35] and Selvam et al. [36]. Similar increase in the wear resistance of the nanocomposite samples fabricated by drop hammer and quasi-static hot pressing for the increased nano reinforcement content can be observed. It is believed that this improvement is directly associated with the increase of hardness and strength of the nanocomposites with reinforcement level. The connection between hardness and wear loss can be explained by Archard's law which describes an inverse proportionality between hardness and the wear rate of a material [37]. The results show that variations of microhardness versus weight loss confirms the Archard's equation. Shanthi et al. [38] and Lim et al. [3] also reported similar findings.

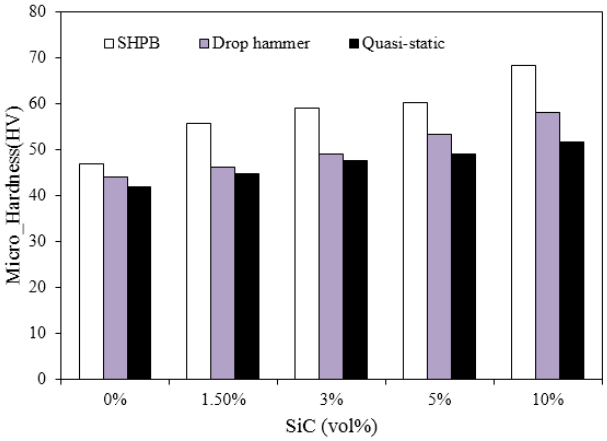

Fig. 5. Variation of microhardness of the top surface vs SiC content.

3.3. Load Effects

Normal interfacial loads in contacting components play a vital role in wear and erosion mechanisms in industry. Therefore, the study of the effects of normal loads on tribological behavior of materials is a requirement [4]. Variation of weight loss versus load at sliding speed of 0.09m/s and different normal loads is shown in Fig. 7. As the figure shows, weight loss increases with the increase of normal load from 10 to 20N for all methods. It is also evident from Fig. 7d that the weight loss of all specimens enhances with the increase in load. The highest rate for the increase is obtained for the quasi static compaction and the lowest rate is obtained for SHPB implying that the rate of weight loss decreases with the increase of strain rate. The increase of weight loss with the increase of the normal load can be attributed to the increased plastic deformation [39]. Fur-

thermore, the addition of SiC nanoparticles to Mg matrix decreases the weight loss due to strong bonding between Mg and SiC particles during consolidation [36]. Considering the applied load of 20N, the reduction of weight loss, as the reinforcement content increases to 10 vol%, is around 63%, 58%, and 35% for the samples fabricated by SHPB, drop hammer, and quasi-static hot pressing, respectively.

Having weight loss for a specific sliding distance, one can simply calculate the wear rate as the ratio of weight loss to sliding distance. Variation of wear rate versus the SiC nano particles content is typically illustrated in Fig. 8 for the sliding distance of 500m and 20N normal load. As the figure indicates, wear rate decreases with increasing nano reinforcement. In addition, compaction with higher densification rates has led to lower wear rates. For example, the wear rate for samples fabricated by SHPB is nearly 40% lower than that for quasi-statically fabricated samples without reinforcement. For Mg-10 vol% SiC samples the reduction of wear rate for SHPB is about 70%. Similar results were reported by Yao et al. [40] for wear resistance of AZ91/TiC composite reinforced with TiC and Lim et al. [3] for AZ91 alloy reinforced with SiC.

3.4. Worn Surface Analysis

As stated before, nano reinforcement could remarkably improve the wear resistance of the samples. In order to investigate this finding more precisely, the worn surfaces were examined using SEM micrographs with EDS analysis. SEM pictures of the worn surfaces of the specimens produced by the high rate compaction methods employed in this work are depicted in Figs. 9 to 11. It is obvious in the figures that as the reinforcing content increases, the wear track becomes smaller and the grooves width decreases . Moreover, the grooves on the samples fabricated by SHPB are narrower and shallower compared with drop hammer and quasi-static compacted samples. These observations are indications of adhesive friction mechanism [41].

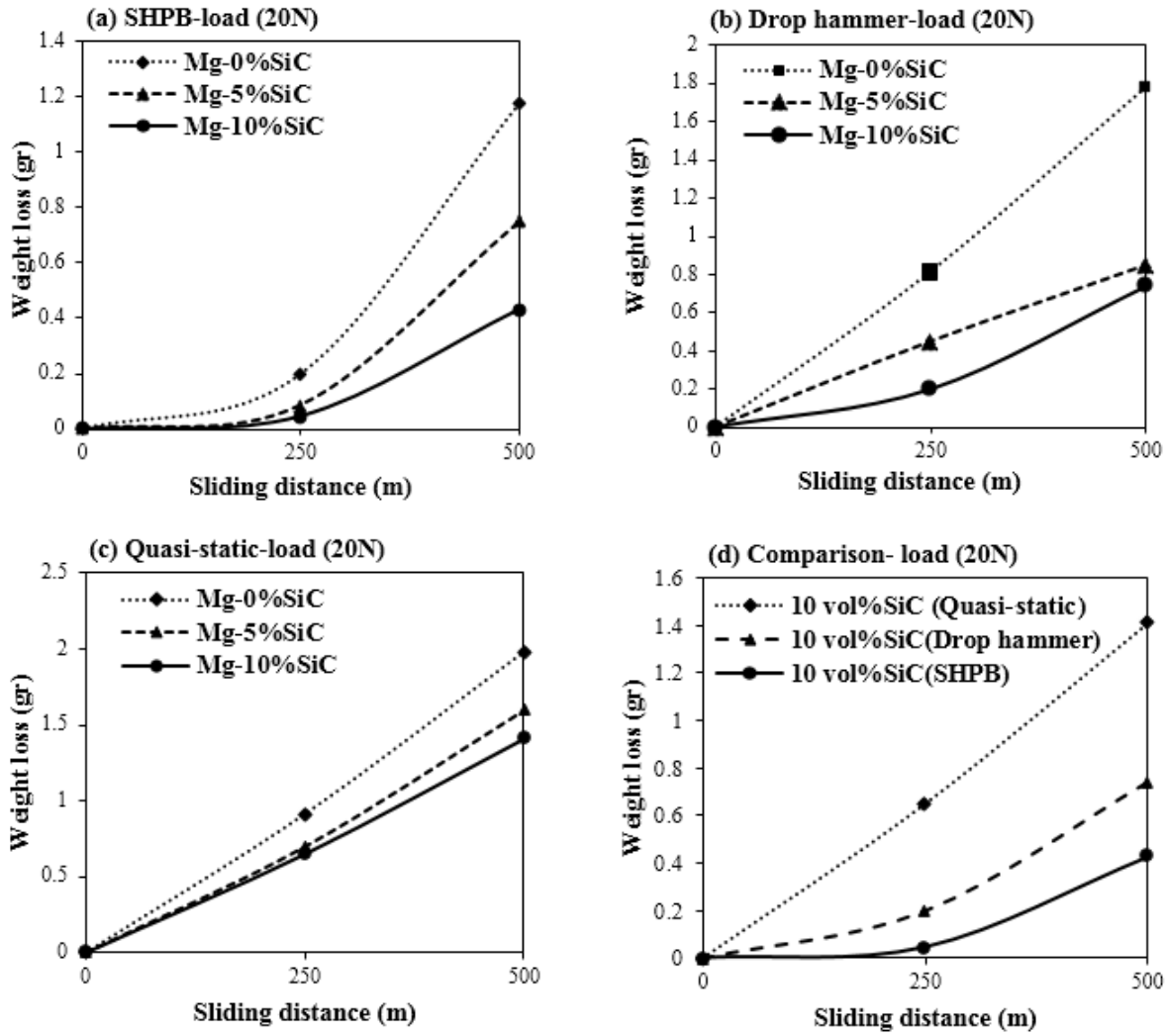

Fig. 6. Variation of weight loss for the applied load of 20N against sliding distance for samples fabricated by (a) SHPB, (b) Drop hammer, (c) Uniaxial quasi-static pressing, (d) A comparative view.

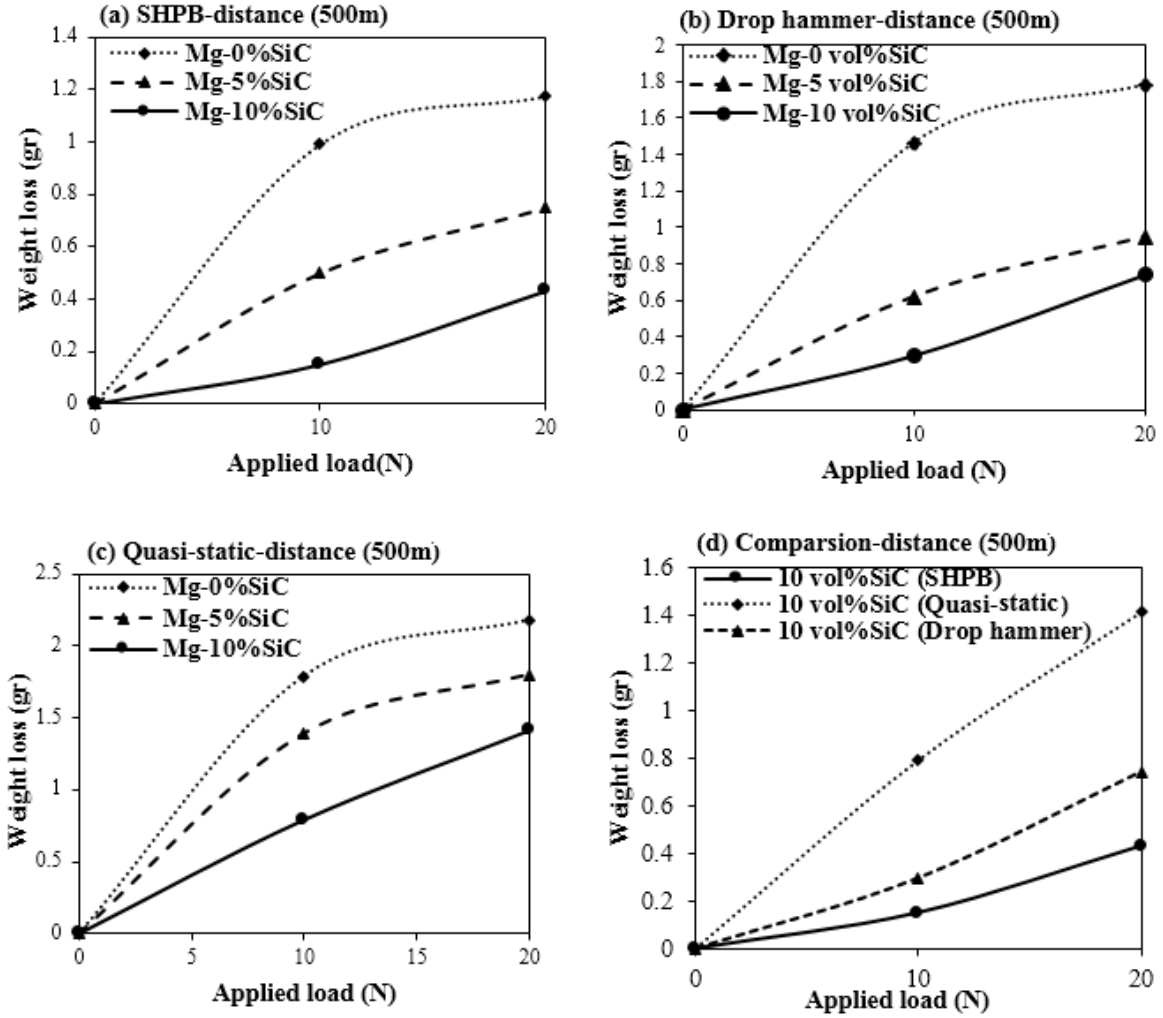

Fig. 7. Variation of wear loss versus the applied load at the sliding distance of 500m for the samples fabricated by: (a) SHPB, (b) Drop hammer, (c) Quasi-static hot pressing, (d) a comparative view.

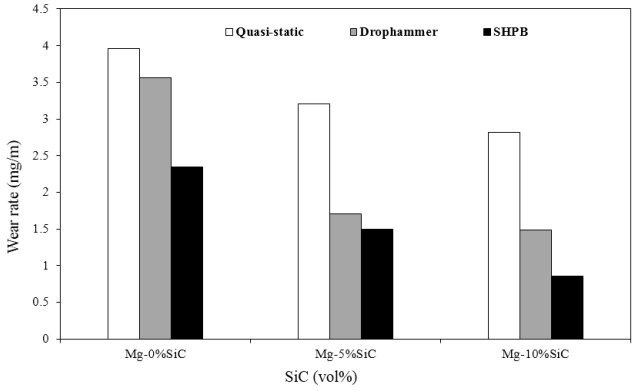

Fig. 8. The effect of SiC vol% on the wear rate under the applied load of 20N and sliding distance of 500m for different fabrication techniques.

A comparison between parts (a) to (c) of each figure (Figs. 9-11) reveals that the quasi-statically compacted samples have more craters and delaminations on their surfaces. These observations imply that the samples fabricated by SHPB have more strength and hardness as well as stronger bonding between Mg and SiC particles [13] and [14].

Actually, for the samples with lower microhardness the counter faces between the pin and the sample surface increase, therefore more materials are detached from the sample's surface. This detachment may be due to adhesive friction that consequently increases the wear rate. Lower wear rate in the samples fabricated by SHPB is traced back to the mild wear with abrasive wear mechanism and shows improved condition for wear behavior [36]. Additionally, nano reinforcements decreased the FC and plastic deformation, therefore they have altered the severe adhesive wear mechanism to the mild abrasive wear (see the continuous and parallel grooves in SHPB samples) [42]. Abrasive wear is due to movement of the high-hardness pin over the low-hardness material, which makes some grooves propagating to the sample surface. Following grooves creation, the material begins to flow, some delamination happens and craters are produced [43]. Higher surface hardness due to nano reinforcement or obtained by higher compaction velocity (fabrication by SHPB, drop hammer and quasi-static hot pressing) reduces adhesion features and converts the wear mechanism to abrasive.

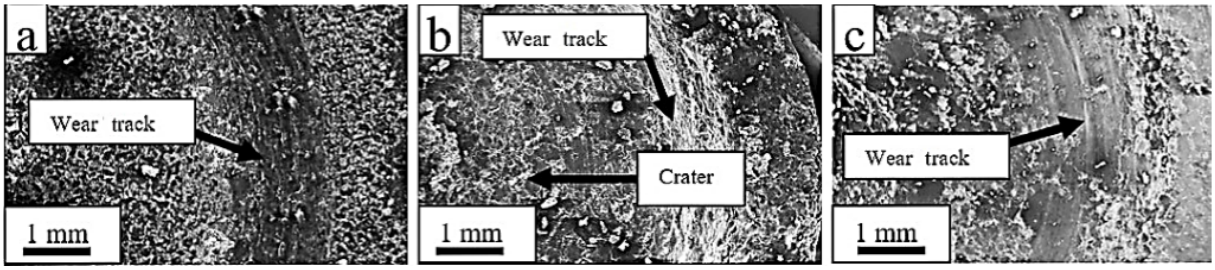

Fig. 9. SEM micrograph of wear track of Mg-0 vol% SiC compacted samples by: (a) SHPB, (b) Drop hammer, (c) Quasi-static hot pressing.

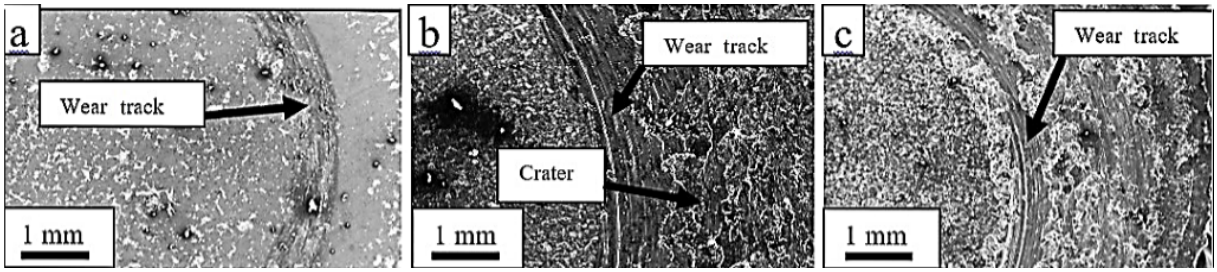

Fig. 10. SEM micrograph of wear track of Mg-5 vol% SiC compacted samples by: (a) SHPB, (b) Drop hammer, (c) Quasi-static hot pressing.

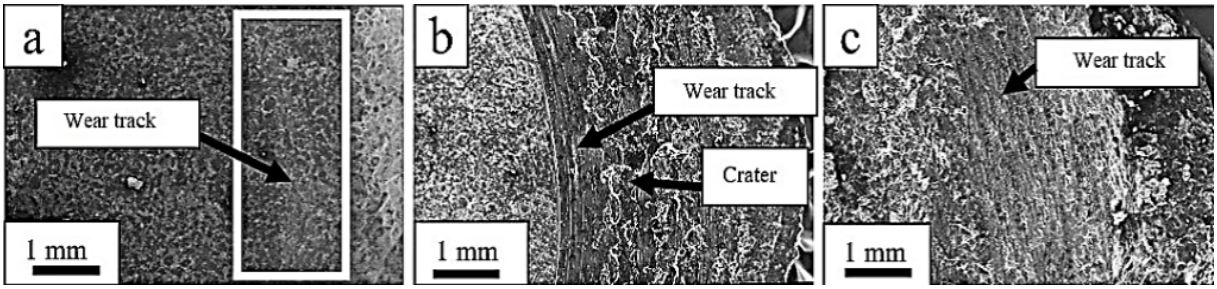

Fig. 11. SEM micrograph of wear track of Mg-10 vol% SiC compacted samples by: (a) SHPB, (b) Drop hammer, (c) Quasi-static hot pressing.

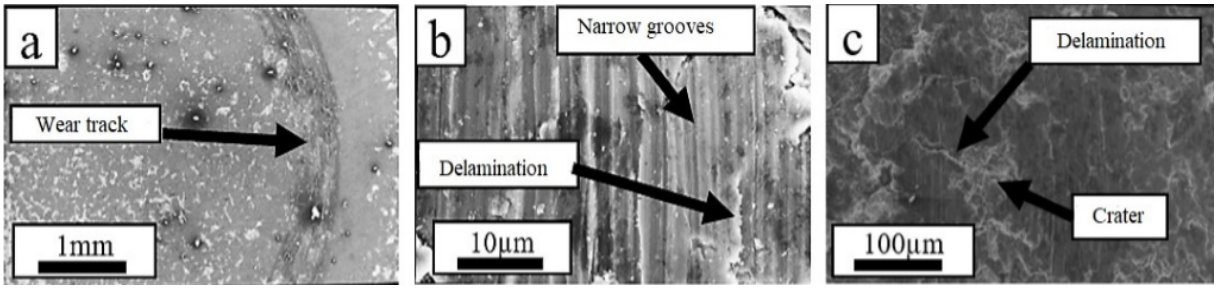

Fig. 12. Wear track of Mg-5% SiC sample fabricated by SHPB for different magnifications.

Fig. 12 shows typical worn surface of a sample (Mg-5 vol% SiC) fabricated by SHPB at different magnifications. Evidences of delamination and deep crater as well as narrow grooves can be seen in Fig. 12 which shows that abrasion and delamination are dominant wear mechanisms in the worn surfaces [27].

Fig. 13 shows the worn debris of samples fabricated by SHPB. As the figure suggests the size of wear debris is reduced when the reinforcing content is increased. As illustrated in part (a) of Figs. 9-11, in the worn surface of Mg-0 vol% SiC more separated and deeper grooves are observed than for Mg-5 vol% SiC and Mg-10 vol% SiC. These features along with plastic deformation indicate adhesive and delamination wear mechanisms [41] in the worn surfaces. Furthermore, the morphology of the worn debris in Fig. 13 a demonstrates adhesive wear mechanism in Mg-0 vol% SiC sample. As mentioned earlier, nanocomposite samples had shallower grooves than Mg-0 vol% SiC which is due to SiC reinforcing particles which enhance the sample hardness. The SiC inclusions also prohibit direct contact of the pin with Mg surface, therefore it reduces the size and population of the worn debris [43].

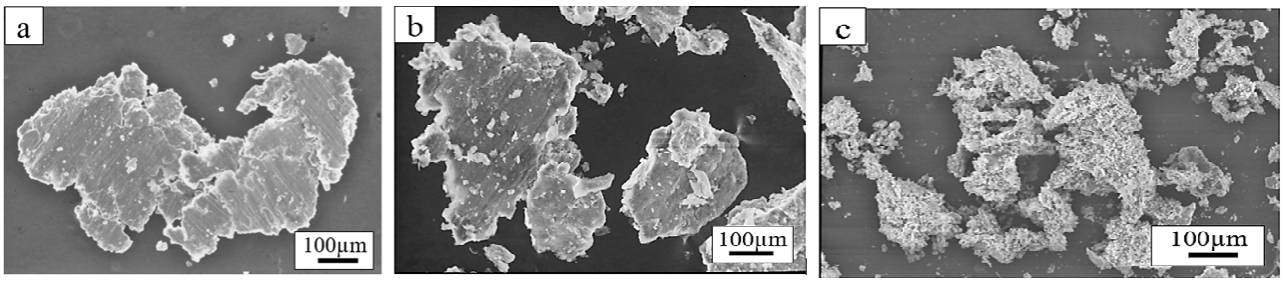

Fig. 13. SEM micrographs of worn debris of samples dynamically compacted by SHPB; (a) Mg, (b) Mg-5 vol% SiC, (c) Mg-10 vol% SiC.

The debris of smaller size are the result of abrasive effect of hard nanoparticles and as a result, higher nanoparticle fraction will cause more and smaller debris (See Figs. 13b and 13c). Therefore, it may be argued that in the nanocomposites having smaller wear debris, compared with the monolithic material, the effect of abrasive mechanism is more profound [9]. EDS point analysis of the worn debris seen in Fig. 13c is presented in Fig. 14. The figure clearly shows very low Fe and Ti contents in the worn debris. The transfer of Fe and Ti from the steel pin to the worn surface is a clear indication that abrasion is one of the dominant wear mechanisms in wear test of samples.

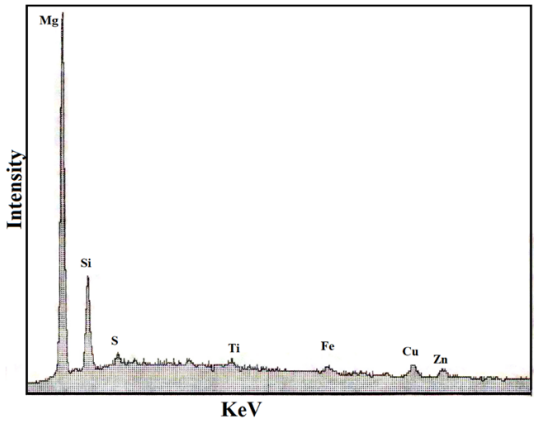

Fig. 14. EDS point analysis of worn debris depicted in Fig. 13c.

3.5. Friction Coefficient

Variation of friction coefficient (FC) versus methods and content reinforcement is presented in Figs. 15 and 16. FC was measured by wear test under the normal load of 20N and the sliding speed of 0.09m/s. Fig. 15 shows the variation of FC for Mg-5 vol% SiC nanocomposites fabricated by different techniques. The severe fluctuations of FC is due to aggregation or removal of worn debris during the test [43]. According to Fig. 15, the FC of Mg-5% SiC nanocomposite samples has decreased from about 0.27 to 0.15 when the production method alters from quasi-static to SHPB. The lower FC for SHPB sample is believed to be due to strong bonding between Mg and SiC nano particles, hardness effects of SiC, and lower tendency to adhesive friction during wear. In general, harder surfaces cause smaller contact area between the pin and the sample surface, consequently, it gives rise to reduction of FC [9]. Umeda et al. [7] and Mohammad-Sharifi et al. [44] also reported similar observations in their investigations. Variation of friction coefficient for nanocomposite samples fabricated by SHPB and under the applied load of 20N for various SiC volume fractions is shown in Fig. 16. As the figure suggests, the average of FC is reduced significantly (around 81%) as the reinforcing content increases from 0 vol% to 10 vol%.

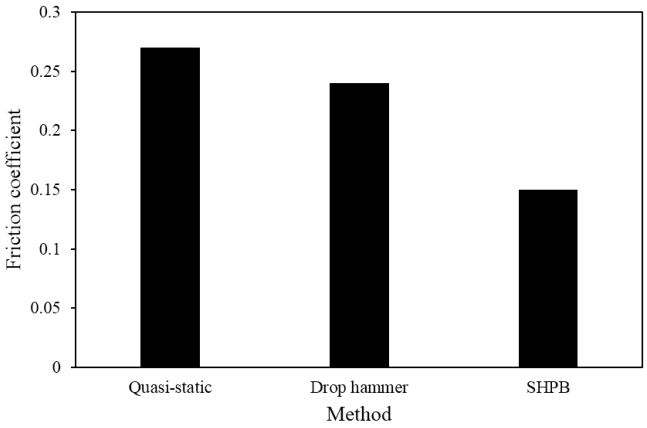

Fig. 15. Variation of friction coefficient of Mg-5 vol% SiC nanocomposites fabricated by different techniques and under applied load of 20N and distance of 500m.

As Fig. 5 demonstrates, 10 vol% SiC nano reinforcement has increased the microhardness significantly (about 45%) which in turn enhances the resistance against plastic deformation of surface layers. Hence, this behavior impedes adhesion of these plastically deformed layers to the surface [43]. Lower FC and wear rate of Mg-10 vol% SiC can also be explained by Archard equation [37]. The largest variation of FC is seen for both the Mg-0 vol% SiC and Mg-5 vol% SiC; the reason is adhesion of wear debris to the surface that increases the surface roughness of the specimens. Moreover, the total wear loss is proportional to the coefficient of friction [42]. It means that both the uniform distribution of SiC hard nanoparticles and strong bonding are effective in improving the tribo-

logical properties of the Mg-SiC nanocomposite by decreasing the FC and wear loss during sliding [45, 46]. Similar to this research, Jafari et al. [42] reported that the average of FC for nanostructured Al2024 sample is much smaller than Al2024-O and Al2024-T6 samples mainly because of the high hardness of the nanostructured alloy. Shanthi et al. [38] also reported similar observations.

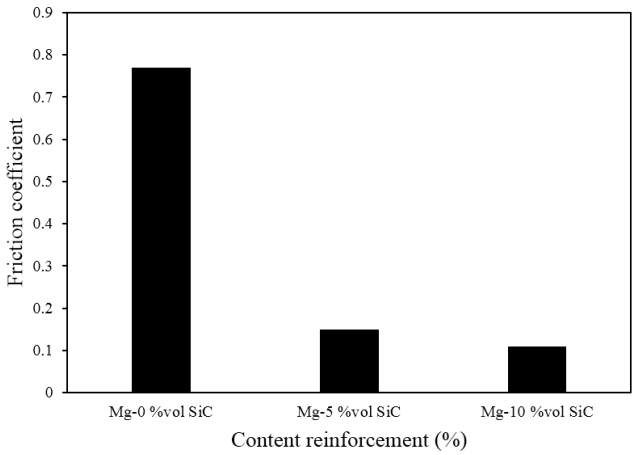

Fig. 16. Variation of friction coefficient for nanocomposite samples fabricated by SHPB and under the applied load of 20N and distance of 500m.

4. Conclusions

Based on the investigations presented in this paper, following concluding remarks may be drawn:

1. Incorporation of 10 vol% SiC reinforcement to Mg matrix improved the Vickers microhardness by about 45% for SHPB method, 32% for drop hammer method, and 24% for quasi_static method.

2. Nano reinforcement could increase the wear resistances of the samples fabricated by quasi-static and dynamic compaction procedures under the normal load of 20N and sliding speed of 0.09m/s. The reduction of weight loss as the reinforcement content increased to 10 vol%, which is near 63%, 58%, and 35% for the samples fabricated by SHPB, drop hammer, and quasi-static hot pressing, respectively.

3. The wear rate of samples fabricated by SHPB was nearly 40% lower than that for quasi-statically fabricated samples and non-reinforced samples, while it was about 70% for Mg-10 vol% SiC samples.

4. SEM observations showed that the samples fabricated by SHPB had higher resistance against surfaces erosions such as scratches and wear.

5. The SEM analysis of the worn surfaces of the specimens showed that the adhesion, abrasive, and delamination were the dominant wear mechanisms.

References

[1] S. Sharma, B. Anand, M. Krishna, Evaluation of sliding wear behaviour of feldspar particle-reinforced magnesium alloy composites, Wear, 241(1) (2000) 33-40.

[2] S.K. Thakur, B.K. Dhindaw, The influence of interfacial characteristics between SiC p and Mg/Al metal matrix on wear, coefficient of friction and microhardness, Wear, 247(2) (2001) 191-201.

[3] C. Lim, S. Lim, M. Gupta, Wear behaviour of SiC p-reinforced magnesium matrix composites, Wear, 255(1-6) (2003) 629-637.

[4] A. Atrian, G. Majzoobi, H. Bakhtiari, The Effect of Pre-compaction on Dynamic Compaction Process of Al/SiC Nanocomposite Powder, The Bi-Annual International Conference on Experimental Solid Mechanics and Dynamics (X-Mech-2014), Tehran (2014).

[5] M. Habibnejad-Korayem, R. Mahmudi, Tribological behavior of pure Mg and AZ31 magnesium alloy strengthened by Al_2O_3 nano-particles, Wear, 268(3-4) (2010) 405-412.

[6] A. Mondal, S. Kumar, Dry sliding wear behaviour of magnesium alloy based hybrid composites in transverse direction, Mater. Sci. Forum, (783-786) (2014) 1530-1535.

[7] J. Umeda, K. Kondoh, H. Imai, Friction and wear behavior of sintered magnesium composite reinforced with CNT-Mg_2Si/MgO, Mater. Sci. Eng. A., 504(1-2) (2009) 157-162.

[8] A. Mandal, B. Murty, M. Chakraborty, Wear behaviour of near eutectic Al–Si alloy reinforced with in-situ TiB_2 particles, Mater. Sci. Eng. A., 506(1-2) (2009) 27-33.

[9] M., Jafari, M., M.H. Abbasi, M.H. Enayati, F. Karimzadeh, Mechanical properties of nanostructured Al2024–MWCNT composite prepared by optimized mechanical milling and hot pressing methods, Adv. Powder. Technol., 23(2) (2012) 205-210.

[10] A. Ahmed, A. Neely, K. Shankar, T. Eddowes, Synthesis, tensile testing, and microstructural characterization of nanometric SiC particulate-reinforced Al 7075 matrix composites, Metall. Mater. Trans. A., 41(6) (2010) 1582-1591.

[11] A. Atrian, S.H. Nourbakhsh, Mechanical behavior of Al-SiCnp nanocomposite fabricated by hot extrusion technique, Int. J. Adv. Des. Manuf. Tech., 11 (2018) 33-41.

[12] S. Sattari, A. Atrian, Effects of the deep rolling process on the surface roughness and properties of an Al-3 vol% SiC nanoparticle nanocomposite fabricated by mechanical milling and hot extrusion, Intl J. Min., Met. Mater., 24(7) (2017) 814-825.

[13] K. Rahmani, G.H. Majzoobi, A. Atrian, A novel approach for dynamic compaction of Mg–SiC nanocomposite powder using a modified Split Hopkinson Pressure Bar, Powder. Metall., 61(2) (2018) 164-177.

[14] G.H. Majzoobi, K. Rahmani, A. Atrian, Temperature effect on mechanical and tribological characterization of Mg-SiC nanocomposite fabricated by high rate compaction, Mater. Res. Exp., 5(1) (2018) 015046.

[15] P. Hernández, H. Dorantes, F. Hernandez, R. Esquivel, D. Rivas, V. Lopez, Synthesis and microstructural characterization of Al–Ni_3Al composites fabricated by press-sintering and shock-compaction, Adv. Powder. Technol., 25(1) (2014) 255-260.

[16] W.H. Gourdin, Dynamic consolidation of metal powders, Prog. Mater Sci., 30(1) (1986) 39-80.

[17] S.K. Thakur, G.T. Kwee, M. Gupta, Development and characterization of magnesium composites containing nano-sized silicon carbide and carbon nanotubes as hybrid reinforcements, J. Mater. Sci., 42(24) (2007) 10040-10046.

[18] E.D. Francis, N. Eswara Parsad, Ch. Ratnam, S.K. Pitta, V.K. Venkata, Synthesis of nano alumina reinforced magnesium-alloy composites, Int. J. Adv. Sci. Tech., 27 (2011) 35-44.

[19] Q. Jiang, H.Y. Wang, B.X. Ma, Y. Wang, F. Zhao, Fabrication of B_4C particulate reinforced magnesium matrix composite by powder metallurgy, J. Alloy. Compd., 386(1) (2005) 177-181.

[20] J.Z. Wang, X.H. Qu, H.Q. Yin, M.J. Yi, X.J. Yuan, High velocity compaction of ferrous powder, Powder. Technol., 192(1-2) (2009) 131-136.

[21] Z. Yan, F. Chen, Y. Cai, High-velocity compaction of titanium powder and process characterization, Powder. Technol., 208(3) (2011) 596-599.

[22] A.N. Faruqui, Mechanical milling and synthesis of Mg-SiC composites using underwater shock consolidation, Met. Mater. Int., 18(1) (2012) 157-163.

[23] A. Atrian, G.H. Majzoobi, H. Bakhtiari, M.H. Enayati, A comparative study on hot dynamic compaction and quasi-static hot pressing of Al7075/SiC np nanocomposite, Adv. Powder. Technol., 26(1) (2015) 73-82.

[24] G.H. Majzoobi, A. Atrian, M.K. Pipelzadeh, Effect of densification rate on consolidation and properties of Al7075–B_4C composite powder, Powder Metall., 58(4) (2015) 281-288.

[25] A. Atrian, G.H. Majzoobi, S.H. Nourbakhsh, S.A. Galehdari, R.M. Masoudi Nejad, Evaluation of tensile strength of Al7075-SiC nanocomposite compacted by gas gun using spherical indentation test and neural networks, Adv. Powder. Technol., 27(4) (2016) 1821-1827.

[26] A. Mondal, S. Kumar, Dry sliding wear behaviour of magnesium alloy based hybrid composites in the longitudinal direction, Wear, 267(1-4) (2009) 458-466.

[27] G. Majzoobi, A. Atrian, M. Enayati, Tribological properties of Al7075-SiC nanocomposite prepared by hot dynamic compaction, Compos. Interface., 22(7) (2015) 579-593.

[28] G. Majzoobi, H. Bakhtiari, A. Atrian, Warm dynamic compaction of Al6061/SiC nanocomposite powders, Proc. Ins. Mech. Eng. L. J. Materi. Des. Appl., 230(2) (2016) 375-387.

[29] Standard, A., E384 (2010e2): Standard test method for Knoop and Vickers hardness of materials. ASTM Standards, ASTM International, West Conshohocken, PA, (2010).

[30] Standard, A., G99-05, Standard Test Method for Wear Testing with a Pin-on-Disk Apparatus, ASTM International, West Conshohocken, PA, (2010).

[31] A. Alizadeh, E. Taheri-Nassaj, Wear behavior of nanostructured Al and Al-B_4C nanocomposites produced by mechanical milling and hot extrusion, Tribol. Lett., 44(1) (2011) 59.

[32] S. Seetharaman, J. Subramanian, K.S. Tun, A.M.S. Hamouda, M. Gupta, Synthesis and characterization of nano boron nitride reinforced magnesium composites produced by the microwave sintering method. Materials, 6(5) (2013) 1940-1955.

[33] Q. Jiang, H. Wang, J.G. Wang, C.L. Xu, Fabrication of TiCp/Mg composites by the thermal explosion synthesis reaction in molten magnesium, Mater. Lett., 57(16-17) (2003) 2580-2583.

[34] M.J. Yi, H.Q. Yin, J.Z. Wang, X.J. Yuan, Comparative research on high-velocity compaction and conventional rigid die compaction, Front. Mater. Sci. China., 3(4) (2009) 447-451.

[35] Z.B. Wang, N.R. Tao, S. Li, W. Wang, G. Liu, J. Lu, Effect of surface nanocrystallization on friction and wear properties in low carbon steel, Mater. Sci. Eng. A., 352(1-2) (2003) 144-149.

[36] B. Selvam, P. Marimuthu, R. Narayanasamy, M. Kamaraj, Dry sliding wear behaviour of zinc oxide reinforced magnesium matrix nano-composites. Mater. Des., 58 (2014) 475-481.

[37] J. Archard, Contact and rubbing of flat surfaces, J. Appl. Physic., 24(8) (1953) 981-988.

[38] M. Shanthi, Q. Nguyen, M. Gupta, Sliding wear behaviour of calcium containing AZ31B/Al_2O_3 nanocomposites, Wear, 269(5) (2010) 473-479.

[39] I. Aatthisugan, A.R. Rose, D.S. Jebadurai, Mechanical and wear behaviour of AZ91D magnesium matrix hybrid composite reinforced with boron carbide and graphite, J. Magnesium Alloys, 5(1) (2017) 20-25.

[40] X. Yao, Z. Zhang, Y.F. Zheng, C. Kong, M.Z. Quadir, J.M. Liang, Y.H. Chen, P. Munroe, D.L. Zhang, Effects of SiC nanoparticle content on the microstructure and tensile mechanical properties of ultrafine grained AA6063-SiCnp nanocomposites fabricated by powder metallurgy, J. Mater. Sci. Technol., 33(9) (2017) 1023-1030.

[41] D. Markov, D. Kelly, Mechanisms of adhesion-initiated catastrophic wear: pure sliding, Wear, 239(2) (2000) 189-210.

[42] M. Jafari, M.H. Enayati, M.H. Abbasi, F. Karimzadeh, Compressive and wear behaviors of bulk nanostructured Al2024 alloy, Mater. Des., 31(2) (2010) 663-669.

[43] S.R. Anvari, F. Karimzadeh, M.H. Enayati, A novel route for development of Al-Cr-O surface nano-composite by friction stir processing, J. Alloy. Compd., 562(Supplement C) (2013) 48-55.

[44] E.M. Sharifi, F. Karimzadeh, M. Enayati, Fabrication and evaluation of mechanical and tribological properties of boron carbide reinforced aluminum matrix nanocomposites, Mater. Des., 32(6) (2011) 3263-3271.

[45] Z. Han, L. Lu, K. Lu, Dry sliding tribological behavior of nanocrystalline and conventional polycrystalline copper, Tribol. Lett., 21(1) (2006) 45-50.

[46] X.R. Lv, S.G. Wang, Y. Liu, K. Long, S. Li, Z.D. Zhang, Effect of nanocrystallization on tribological behaviors of ingot iron, Wear, 264(7-8) (2008) 535-541.